PCCP

Accepted Manuscript

ROYAL SOCIETY OF CHEMISTRY

rsc.li/pccp

View Article Online
DOI: 10.1039/C7CP08231B

PCCP

ARTICLE

Atomic Structure and Electronic Properties of A_2B_2XY (A = Si-Pb, B = Cl-I, and XY = PN and SiS) Inorganic Double Helices: First Principles Calculations

Received 00th January 20xx,
Accepted 00th January 20xx

DOI: 10.1039/x0xx00000x

www.rsc.org/

T.K. Bijoy[a,b$], P. Murugan[b,c] and Vijay Kumar[a,d$*]

We study the structural stability and electronic properties of new classes of DNA-like inorganic double helices of the type A_2B_2XY (A = Si-Pb, B = Cl-I, and XY = PN and SiS) by employing first principles density functional theory (DFT) calculations including van der Waals interactions. In these quaternary double helices PN or SiS forms the inner helix while the AB helix wraps around the inner helix and the two are interconnected. We find that the bromides and iodides of Ge, Sn, and Pb as well as Pb_2Cl_2PN form structurally stable double helices while Ge_2I_2SiS as well as bromides and iodides of Sn and Pb have stable double helices. The atomic structures of different double helices have been analyzed in detail to understand the stability of these systems as there is up to about 80% difference in the interatomic distances in the two helices which is remarkable. Also in these new classes of double helices there is polar covalent bonding in the inner helix due to heteroatoms. We have calculated the DDEC6 partial atomic charges and bond orders which suggest strong covalent bonding in the inner helix. The electronic structure reveals that these double helices are semiconducting and in many cases the band gap is direct. Further we have studied the effects of doping and it is found that the hole doping is the most appropriate way for tuning their electronic properties.

Introduction

The double helical structure of DNA is one of the most important structural units present in the chromosomes of all living being and is among the greatest scientific achievements ever made[1]. This double helix structure has also motivated materials scientists to mimic and synthesize similar structures for new functional materials. In this direction, several efforts have been made for artificially regenerating such systems and some organic polymers having helical structure like that of DNA have been synthesized[2-4]. Still replicating biological systems is a tedious task due their complex structure characteristics. Very recently inorganic double helices of halides of group 14 elements such as Si, Ge, and Sn have been reported. These double helices of SnIP type have an inner helix of P as core and an outer helix of SnI[5]. The two are interconnected. The electronic structure of these one dimensional structures shows them to be semiconducting and therefore such structures could be promising for devices and optoelectronic applications at the nanoscale[6,7]. Interestingly these inorganic double helices are devoid of carbon and open up new avenues for inorganic semiconducting nanomaterials. An understanding of their stability is very desirable to explore new systems.

Prior to the finding of SnIP type double helices, there are reports of the formation of a double helix structure in a binary system having Li and P atoms[8-10]. Here, we explore the formation of double helices in quaternary systems with a heteroatomic inorganic inner helix while the outer helix is made of IV-VII combination as in SnIP. To achieve this, we replaced the P chain of the inner

[a]Dr. Vijay Kumar Foundation, 1969 Sector 4, Gurgaon 122001, Haryana, India *Email:kumar@vkf.in and vijay.kumar@snu.edu.in
[b]Academy of Scientific and Innovative Research (AcSIR)-CSIR-Central Electrochemical Research Institute, Karaikudi 630003, Tamil Nadu, India
[c]Functional Materials Division- CSIR-Central Electrochemical Research Institute, Karaikudi 630003, Tamil Nadu, India
[d]Center for Informatics, School of Natural Sciences, Shiv Nadar University, NH-91, Tehsil Dadri, Gautam Buddha Nagar 201314, Uttar Pradesh, India
[$] These authors contributed equally

Supplementary Information.
1) Fig. S1 gives the atomic structure of SnIP double helix.
2) Fig. S2 gives the atomic structures of (a) Ge_2Br_2PN, (b) Sn_2Cl_2PN, (c) Sn_2Br_2PN, (d) Pb_2Cl_2PN, and (e) Pb_2Br_2PN double helices.
3) Fig. S3 gives the total and partial (angular momentum resolved) electronic densities of states of (a) Ge_2Br_2PN, (b) Sn_2Cl_2PN, (c) Sn_2Br_2PN, (d) Pb_2Cl_2PN, and (e) Pb_2Br_2PN double helices.
4) Fig. S4 gives the electronic band structures of Ge_2Br_2PN, Sn_2Cl_2PN, Sn_2Br_2PN, Pb_2Cl_2PN and Pb_2Br_2PN double helices.
5) Atomic coordinates of the structures, the charges on atoms and the bond order are given.

ARTICLE PCCP

View Article Online
DOI: 10.1039/C7CP08231B

helix by an inorganic hetero-chain such as PN and SiS. It is to be noted that PN is well known for its ability to form polymeric chains while SiS chain is electronically equivalent to P chain[11-13]. Also as 2D materials, IV-VI compounds have been attracting much attention recently because they form layered structures similar to phosphorene[14-17]. The Si-S bond length is also similar to that of the P-P bond. These factors make SiS as a suitable candidate for substitution in place of the P chain. However, as we shall show, in SnIP double helix there is some charge transfer to P atoms while in PN inner helix, charge transfer occurs from P to N atoms. Also in the case of SiS inner helix, charge transfer occurs from Si to S atoms. Accordingly, the stability of A_2B_2XY double helices is also an indicator of the tolerance of these structures for charge adjustment. Our results suggest that among A_2B_2PN double helices, bromides and iodides of Ge, Sn, and Pb as well as Pb_2Cl_2PN are stable while chlorides of Si and Ge are structurally not stable. On the other hand bromides and iodides of Sn and Pb as well as Ge_2I_2SiS form stable double helices with SiS inner helix. We have further explored the tuning of the electronic properties of these 1D semiconducting structures by studying effects of doping. Our results suggest that hole doping is the best way for enhancing their electronic conductivity.

Computational Methodology

We have performed first principles calculations using density functional theory to understand the structural and electronic properties of A_2B_2XY type double helices. The electron-ion interactions have been treated using projector augmented wave (PAW)[18] pseudopotential method in Vienna Ab-initio Simulation Package (VASP)[19,20]. The exchange-correlation energy has been calculated using PW91 generalized gradient approximation (GGA)[21]. For these helical nanowires, periodicity is maintained along the z-direction and sufficient vacuum space of approximately 12 Å has been kept along x and y directions in order to avoid interaction of the double helix with its periodic images. The presence of a diatomic inner helix leads to doubling of the unit cell compared with the SnIP case and there are 42 atoms (14 each from group 14 elements and halogens while the inner helix contains 14 atoms seven atoms each of P and N or Si and S). For the plane wave expansion of the wavefunction, a cut-off energy of 400 eV has been used. The Brillouin zone has been sampled using 1×1×4 **k**-points mesh for optimizing the atomic structure of the helices but a dense **k**-points mesh of 1×1×50 has been used to plot the energy bands and the electronic density of states (DOS). Throughout the geometry optimization calculations, all the ions were relaxed without considering any symmetry and the iterative relaxation process was repeated until the absolute value of the force on each ion was converged to less than 0.01 eV/Å. The convergence for energy was set to 10^{-5} eV. In addition, we repeated all calculations with spin-polarization to check if these systems have magnetic solution but our results suggest that the helices are non-magnetic. Further we performed calculations by considering van der Waals (vdW) interactions as weak interactions are expected between turns of the helices even though within the helices the interactions are predominantly covalent or polar covalent. We followed the method of Tkatchenko and Scheffler[22,23] with PBE[24] exchange-correlation functional within GGA and optimized the structures fully with high precision. Our results suggest that there is a small reduction (about 0.25%) in the lattice parameter along the z-axis in all cases. Therefore, the results of the atomic structure and energy bands are given without vdW interactions. However, there is significant contribution to the cohesive energy and these are included in our results. Furthermore we have performed Bader charge analysis[25,26] by calculating the all electron charge density. Also we have used Chargemol program[27,28] to obtain the DDEC6 net atomic charges and bond orders.

Results and discussion

To begin with we modelled and optimized a SnIP double helix. The optimized atomic structure shows that the double helix is stable and our results (see Table 1) are consistent with the previous reports. Structurally, in SnIP double helix, SnI forms the outer helix and P atoms form the covalently bonded inner helix as shown in Fig. S1 (refer Supplementary Information). The average Sn-I and P-P bond distances in this double helix differ a lot and are

PCCP ARTICLE

View Article Online
DOI: 10.1039/C7CP08231B

3.17 Å and 2.20 Å, respectively, while the Sn-P bond length is 2.73 Å. An important observation is that the bond distances in the outer helix are much longer than in the inner helix which is very unusual when one considers that in alloy formation normally a maximum of about 15% variation is taken as a limit for mixing. The tetravalent Sn atom in the outer helix is coordinated with two I atoms in the same helix and two P atoms of the inner helix. Similar calculations by taking Si and Ge in place of Sn, and replacing I with Cl or Br show that these double helices are also stable as reported earlier[6]. Subsequently we considered 1D strands of A_2B_2PN and A_2B_2SiS type with A = Sn-Pb and B = Cl-I, by replacing the inner helix of P by a heteroatomic chain, namely PN and SiS. PN chains are well known for a long time in the field of inorganic polymers since P and N are capable of forming a variety of polymers together[11,12] and SiS is considered due to its electronic equivalence with P. As we shall show, the stability of the inorganic double helix structure depends on the relation between the interatomic bond lengths in the two helices. The P-N bond length (1.77 Å) is comparatively shorter than that of the P-P bond (2.20 Å) while the SiS bond length (~2.28 Å) is slightly longer than the P-P bond length. Also in contrast to covalent bonding in P inner helix, there is polar covalent bond in PN and SiS helices. Accordingly, the stability of the studied helices also suggests the tolerance for variation in the interatomic distances and charge in the structure.

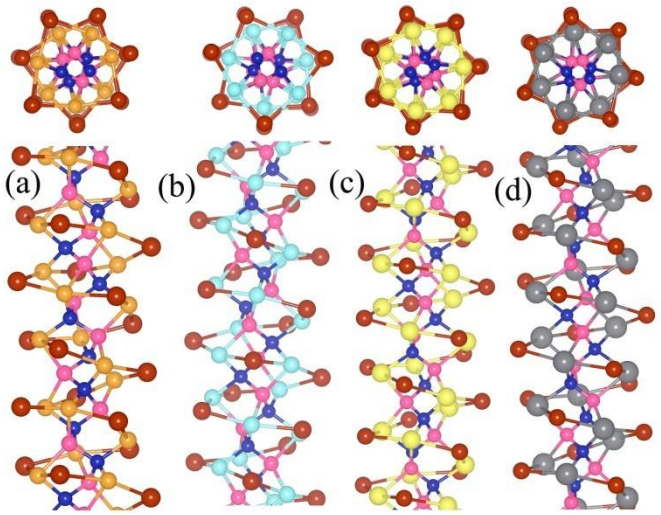

Fig. 1. Top and side views of the ground state structures of the double helices of (a) Si_2I_2PN, (b) Ge_2I_2PN, (c) Sn_2I_2PN, and (d) Pb_2I_2PN. Pink and blue balls represent the inner PN helix while brown, orange, cyan, yellow, and grey balls show I, Si, Ge, Sn, and Pb atoms in the outer helix, respectively. Similar structures have also been obtained for bromides of Ge, Sn, and Pb as well as for chloride of Pb.

The optimized atomic structures of the systems which form stable double helices are shown in **Fig. 1** and **Fig. S2** in the Supplementary Information. In the A_2B_2PN double helix structure, AB forms the outer helix while PN, the inner helix. The structural characteristics of all these systems are given in Table 1 which shows that in going from Si to Pb, the lattice parameter is slightly increased. However, there is not much deviation in the lattice parameter when one halogen is replaced by another (see Table 1). Si_2Cl_2PN and Ge_2Cl_2PN are found to have significant distortions from the double helix structure, whereas other systems form well-ordered stable double helices and each group 14 atom (A) in the outer helix interacts with adjacent P and N atoms of the inner helix. These bonds become slightly elongated as one moves from Cl to I. The halogen atoms in the outer helix do not form a bond with the PN inner helix. Thus all the N and P atoms are tetrahedrally coordinated such that each atom forms bonds with two neighbouring atoms of the inner helix and two bonds with A atoms of the outer helix. The nearest neighbour P-N bond length lies in the range of 1.76-1.82 Å for various double helix structures. However, for Si_2Cl_2PN and Ge_2Cl_2PN which have significantly distorted structures, the Si-Cl and Ge-Cl bonds surrounding the PN chain are non-uniform and have large variation in their bond lengths (2.4-3.2 Å and 2.6-3.3 Å, respectively).

To get a deeper insight regarding the geometrical factors that may lead to the stabilization of double helices, we calculated the ratio *D* of A-B bond length in the outer helix and X-Y (P-N or Si-S) bond length in the inner helix and the values are given in Table 1. The calculated *D* values for A_2B_2PN lie in the range of 1.57 to 1.84. For the system which does not form a stable double helix, the *D* value is comparatively low such as 1.46 for Si_2Cl_2PN. It is noted that *D* increases gradually as we move from Si to

ARTICLE PCCP

View Article Online
DOI: 10.1039/C7CP08231B

Pb or Cl to I. This is due to the increase in the corresponding bond distances. The maximum *D* value of 1.84 has been obtained in the case of Pb_2I_2PN double helix (refer Table 1). In general for symmetric double helices, the *D* value is comparatively higher. In addition to A_2B_2PN helices, we modelled other double helices in which the inner helix is replaced by a SiS heteroatomic helix. IV-VI compounds are electronically equivalent to group 15 elements. Recent studies[15] demonstrate that in two dimensions, SiS and SnS layers structurally mimic phosphorene. With this intuition we replaced P helix by SiS helix. Moreover, since both Si and S are adjacent to P, their atomic sizes are nearly the same and hence the SiS helix will be geometrically approximately the same as the P helix. This is evident from the result that SiS bond length is only slightly larger than that of P-P. This will reduce the size mismatching effect. From the relaxed structures of A_2B_2SiS systems we find that the Cl containing structures show larger deviation from the double helix geometry. For instance in the case of Si_2Cl_2SiS, the outer SiCl helix has Si and Cl atoms separated by a distance ranging from 2.4 to 3.4 Å. However, the double helix structure is preferred for Ge_2I_2SiS, Sn_2Br_2SiS, Sn_2I_2SiS, Pb_2Br_2SiS, and Pb_2I_2SiS.

Table1. Lattice constant along the double helix, A-B and X-Y (PN or SiS) bond lengths, ratio *D* of the A-B and X-Y bond lengths, bond angles (θ_1 and θ_2 with θ_1 = ∠A-B-A and θ_2 = ∠B-A-B as well as φ_1 and φ_2 with φ_1 = ∠P-N-P/∠Si-S-Si and φ_2 = ∠N-P-N/∠S-Si-S), cohesive energy (E_c), and band gap (E_g) of different systems we have studied using PW91-GGA. For SnIP, $\varphi_1 = \varphi_2$ = ∠P-P-P. Values of E_c calculated using PBE functional including vdW correction and the contribution of the vdW correction per atom (ΔE in parenthesis) are also given. * means that the band gap is direct.

System	Lattice constant (Å)	A-B (Å)	X-Y (Å)	*D*	θ_1 (°)	θ_2 (°)	φ_1 (°)	φ_2 (°)	E_c (eV/ Atom)	E_c (eV/atom) with PBE-vdW	E_g (eV)
SnIP	8.04 (8.04)	3.17	2.20	1.44	102.3	157.5	93.9	93.9	3.04	3.08 (0.13)	-
Si_2I_2PN	13.74 (13.61)	2.91	1.82	1.60	88.9	165.4	99.3	95.8	3.45	3.45 (0.10)	0.73*
Ge_2Br_2PN	14.00 (13.95)	2.80	1.78	1.57	97.4	159.4	101.3	97.6	3.67	3.48 (0.08)	1.18
Ge_2I_2PN	14.10 (14.00)	3.00	1.79	1.67	90.0	166.0	101	98.1	3.34	3.34 (0.10)	0.99
Sn_2Cl_2PN	14.59 (14.49)	2.80	1.77	1.58	105.9	151.8	100.7	102.6	3.59	3.61 (0.09)	0.90*
Sn_2Br_2PN	14.61 (14.53)	2.94	1.77	1.66	100.0	157.3	102.3	101	3.45	3.44 (0.10)	0.63
Sn_2I_2PN	14.65 (14.59)	3.16	1.77	1.79	92.3	164.7	102	101.6	3.28	3.28 (0.11)	0.57*
Pb_2Cl_2PN	14.82 (14.75)	2.89	1.76	1.65	105.0	153.0	103.7	101.9	3.58	3.57 (0.09)	0.74
Pb_2Br_2PN	14.82 (14.77)	3.03	1.76	1.73	99.7	158.0	103.3	102.4	3.42	3.43 (0.10)	0.68
Pb_2I_2PN	14.99 (14.94)	3.23	1.76	1.84	92.3	165.1	103.1	103	3.26	3.27 (0.12)	0.64*
Ge_2I_2SiS	15.56 (15.51)	3.07	2.30	1.33	101.8	157.4	98.9	88.4	3.21	3.23 (0.11)	1.17
Sn_2Br_2SiS	16.50 (16.34)	3.0	2.28	1.31	111.3	148.0	101.3	90.8	3.30	3.32 (0.11)	1.04*
Sn_2I_2SiS	16.259 (16.25)	3.18	2.28	1.40	104.7	154.4	99.6	91.0	3.15	3.19 (0.13)	0.88
Pb_2Br_2SiS	16.85 (16.68)	3.09	2.27	1.36	110.8	148.6	102	92.3	3.28	3.30 (0.12)	1.04*
Pb_2I_2SiS	16.61 (16.53)	3.26	2.27	1.44	104.3	154.8	100.3	92.6	3.13	3.18 (0.14)	0.86

PCCP ARTICLE

View Article Online
DOI: 10.1039/C7CP08231B

The optimized structures of these systems are shown in **Fig. 2**. Similar to P and N of the A_2B_2PN helices, here also both Si and S are tetrahedrally coordinated. The Si-S bond length varies from 2.27 Å to 2.30 Å (see Table 1). As in the case of other double helices, the halogen atoms in the outer helix do not make any bond with the inner SiS helix.

Due to the increase in the inner helix (Si-S) bond length, the calculated values of *D* reduce to 1.31-1.44 range compared with the values for the A_2B_2PN systems. But these values are quiet similar to the value of 1.44 for SnIP type double helix (see Table 1). It is worthy to mention that for these helices, ∠ A-B-A in the outer helix is comparatively larger than in the case of A_2B_2PN systems; while ∠ B-A-B is found to be slightly smaller (refer Table 1). Also the lattice parameter increases significantly compared to the values in the case of A_2B_2PN systems. The values of E_c for the A_2B_2SiS double helices are slightly lower than for the A_2B_2PN systems, but they show a similar variation as the halogen atom is changed from Cl to I as shown in **Fig. 3**.

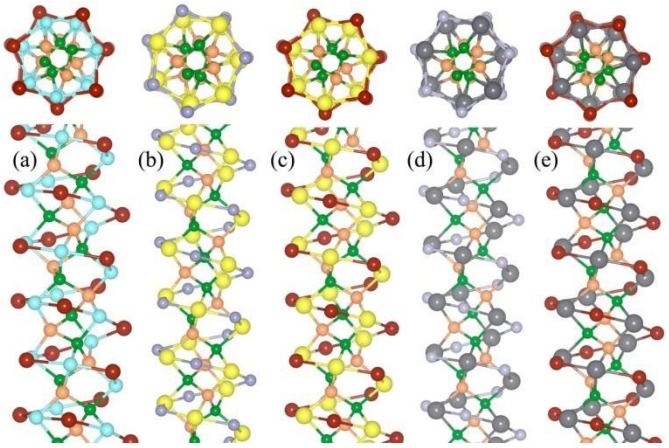

Fig. 2. Top and side views of the optimized atomic structures of (a) Ge_2I_2SiS, (b) Sn_2Br_2SiS, (c) Sn_2I_2SiS, (d) Pb_2Br_2SiS, and (e) Pb_2I_2SiS double helices. Brown, cyan, yellow, and grey balls represent I, Ge, Sn, and Pb atoms, respectively in the outer helix while orange and green ball represent Si and S atoms in the inner helix, respectively.

In order to further understand the structural characteristics of the double helices, we calculated the bond angles of the inner and outer helices and all these values are listed in Table 1. Due to the presence of two types of atoms in the inner helix, there are two possible types of bond angles for the PN (SiS) helix and they are ∠P-N-P (∠Si-S-Si) and ∠N-P-N (∠S-Si-S). As Table 1 shows, in all the cases ∠P-N-P is > ∠N-P-N and both these values increase as we move from Si to Pb. Likewise for the outer helix (AB) we measured ∠A-B-A and ∠B-A-B to understand the atomic orientation within this helix as bond angles decide the curvature of the helix. In all the double helical structures we have studied, it is found that the ∠B-A-B is always much larger than ∠A-B-A. It is worth to mention that with respect to the change in halogen atom, the bond angles vary significantly. The ∠B-A-B is higher for the helices having I atoms. One can further see from the results in Table 1 that ∠A-B-A and ∠B-A-B vary in opposite ways to each other as the halogen atoms are changed. This could help to maintain the curvature of the outer helix.

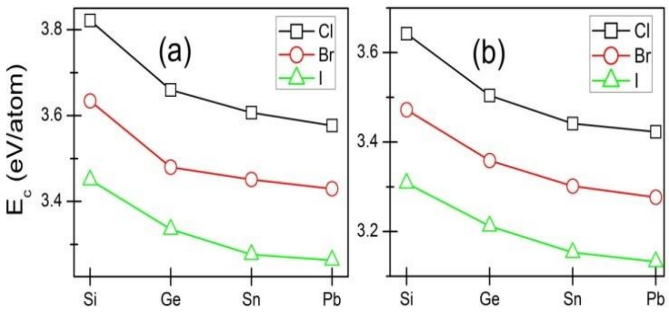

Fig. 3. Cohesive energy for (a) A_2B_2PN and (b) A_2B_2SiS (A = Si – Pb, and B = Cl – I) double helices calculated using PW91-GGA.

In general these systems and also the previously studied SnIP type systems have two length scales: 1) a short one for the inner helix and 2) a long one related to Sn-I type bonds in the outer helix while the bonds between the two helices lie in the intermediate range. The difference between the two lengths is quite large with the largest being about 80% for Pb_2I_2PN (Pb-I bond length 3.23 Å vs. P-N bond length of 1.76 Å). This seems to be a reason that there are two helices and they are interlinked. The latter puts a constraint on which type of helices can coexist as we find from bond lengths and bond angles. A facilitating factor is that there is some flexibility in the structure as the ratios of the two bond lengths in

View Article Online
DOI: 10.1039/C7CP08231B

different systems and to a lesser extent the bond angles suggest. The ratio of the bond lengths vary in the range of 1.31 to 1.84 depending upon the combination of the inner and outer helices that we have studied. This suggests deviation of about 17% from the mean value of 1.575 for *D*. However, we find that the bond angles show less flexibility. The ∠ A-B-A has a mean value of about 100° with ~10% variation while the mean value of the ∠ B-A-B is 158° with ~6% deviation. On the other hand the ∠ X-Y-X and ∠ Y-X-Y have the mean value of 101° with about 2% deviation and 96° with about 7% deviation, respectively. Accordingly the outer helix has more flexibility while the inner helix has strong covalency with less deviation in bond angles.

In order to further understand the energetic stability of the double helices, we have calculated the cohesive energy per atom (E_c) using the following formula,

$$Ec = \frac{n[2E(\mathrm{A}) + 2E(\mathrm{B}) + E(\mathrm{X}) + E(\mathrm{Y})] - E(\mathrm{A_2B_2XY})}{N} \quad (1)$$

Here *E(*A*), E(*B*), E(*X*),* and *E(*Y*)* represent the atomic energies of individual atoms while *E(*A_2B_2XY*)* is the total energy of the double helix; *n* and *N* correspond to the number of formula units in the unit cell and the total number of atoms present in the double helix, respectively.

The E_c for all the studied systems calculated within PW91-GGA is shown in **Fig. 3** and the values are also given in Table 1. Also we have given the values of E_c calculated with PBE by including vdW contributions as well as the vdW contribution (ΔE) in Table 1. We find that both the functional give very similar results. There is a gradual reduction in the value of E_c when either A changes from Si to Pb, or B is varied from Cl to I. Even though Si_2Cl_2PN is a distorted helix, the E_c value is found to be the highest. Also our calculated values of the E_c in quaternary systems are higher compared to the calculated value of 3.04 eV/atom for the previously reported SnIP double helix. Therefore, by replacing covalently bonded P helix by a heteroatom PN helix, the overall E_c can be enhanced, which ultimately improves the thermodynamic stability of the system. Calculations performed by including vdW interactions show that the optimized atomic structures have only a slight reduction (~0.3%) in the lattice parameter along the double helix and the cohesive energy of the double helix increases by about 0.1 eV/atom as it can be seen from Table 1.

From the above results of A_2B_2PN and A_2B_2SiS double helices, we conclude that these systems are capable of forming double helical structures even though the inner helix (PN and SiS) has slightly lower or higher bond length than P inner helix in the case of SnIP. It is important to mention that the change in the inner helix structurally does not affect the outer helix significantly; and therefore the outer helix is slightly flexible in this geometry. The variations in bond angles and *D* value in each system indicate that both the inner and the outer helices of the double helix adjust themselves so that they can interact with each other tetrahedrally.

Table 2. The charge (Q) on each atom as obtained from the DDEC6 (Bader) charge analysis using PBE-GGA with vdw correction. + and – values of Q refer to charge transfer from and to the atom, respectively. The overall trend from the two methods is similar, though the DDEC6 atomic charges are smaller in magnitude than the Bader atomic charges.

System	Atom A Q_A (e)	Atom B Q_B (e)	Atom X Q_X (e)	Atom Y Q_Y (e)
SnIP	+0.39(+0.80)	-0.31(-0.49)	-0.09(-0.31)	-
Si_2I_2PN	+0.19(+0.98)	-0.15(-0.36)	+0.29(+0.63)	-0.38(-1.87)
Ge_2Br_2PN	+0.41(+0.88)	-0.31(-0.51)	+0.24(+0.93)	-0.44(-1.66)
Ge_2I_2PN	+0.34(+0.78)	-0.25(-0.41)	+0.23(+0.91)	-0.43(-1.66)
Sn_2Cl_2PN	+0.55(+1.05)	-0.42(-0.66)	+0.20(+0.91)	-0.48(-1.71)
Sn_2Br_2PN	+0.50(+0.97)	-0.36(-0.58)	+0.19(+0.92)	-0.47(-1.70)
Sn_2I_2PN	+0.43(+0.91)	-0.30(-0.49)	+0.19(+0.88)	-0.46 (-1.71)
Pb_2Cl_2PN	+0.68(+0.97)	-0.49(-0.65)	+0.14(+1.03)	-0.51(-1.66)
Pb_2Br_2PN	+0.62(+0.91)	-0.44(-0.59)	+0.14(+1.0)	-0.50(-1.66)
Pb_2I_2PN	+0.53(+0.83)	-0.35(-0.50)	+0.15(+1.01)	-0.50(-1.68)
Ge_2I_2SiS	+0.25(+0.56)	-0.23(-0.41)	+0.08(+0.74)	-0.12(-1.06)
Sn_2Br_2SiS	+0.43(+0.80)	-0.36(-0.58)	+0.02(+0.67)	-0.15(-1.11)
Sn_2I_2SiS	+0.36(+0.73)	-0.30(-0.49)	+0.01(+0.64)	-0.14(-1.11)
Pb_2Br_2SiS	+0.55(+0.77)	-0.45(-0.60)	-0.02(+0.75)	-0.18(-1.09)
Pb_2I_2SiS	+0.48(+0.71)	-0.38(-0.51)	-0.03(+0.71)	-0.18(-1.10)

In order to further understand the bonding nature in these double helices we calculated the charge transfer by performing Bader charge analysis as well as using DDEC6 net atomic charge and the values are given in Table 2. For comparison we also calculated Bader charge as well as DDEC6 atomic charge for SnIP. The Bader charge shows that each Sn atom in the outer helix gives approximately 0.8 e while each I atom in the outer helix gains nearly 0.49 e and the P atom in the inner helix receives 0.31e. This is due to the higher electronegativity of iodine than P atom. This charge transfer from the outer to the inner helix results in an attractive interaction between the inner and outer helices besides the formation of Sn-P bonds which bind the helices together. In the newly proposed double helices also we find charge transfer from A atoms to B atoms as well as to the inner helix. But additionally there is polar bonding character in the inner helix as charge transfer also occurs from P to N as well as from Si to S atoms. We find that the charge transfer to N and S atoms is about 1.68 e and about 1.1 e, respectively using Bader charge analysis. However, using DDEC6 net atomic charge method, the charge transfer is much less as it can be seen from Table 2, though in the case of the halogen atoms the difference in the values is less. So unlike the covalently bonded P helix in SnIP, there is covalent polar bonding character in the inner heteroatom helix for A_2B_2XY systems.

Figure 4 shows the total and angular momentum resolved electronic density of states (DOS) for A_2I_2PN helices while the results for other systems are given in **Fig. S3** in Supplementary Information. Our results suggest that all the A_2B_2PN double helices including the distorted ones are semiconducting. The GGA band gap of the double helices ranges from 0.58 eV to 1.29 eV (see Table 1). The actual band gap is expected to be higher as in GGA it is underestimated. However, the overall trends are expected to remain similar. The band gap of the double helix gradually decreases in moving from systems having Cl to those having I atoms. In the occupied region, near the valence band maximum, the states arise mainly from the *p* orbitals of halogens and there is some contribution from the *p* orbitals of group 14 atoms.

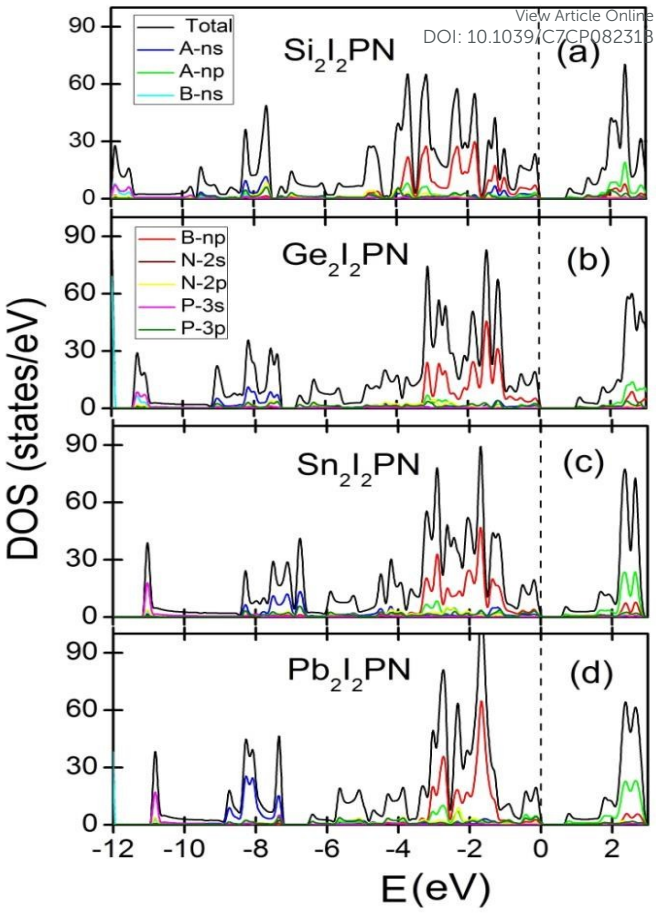

Fig. 4. The total and angular momentum resolved partial electronic density of states of various A_2B_2PN double helices. The vertical broken line shows the top of the valence band.

In general the DOS arising from *ns* (*n* = 3, 4, 5, 6 for Si, Ge, Sn, and Pb, respectively) orbitals of atom A is spread in the range of -9 eV to -7 eV. In the unoccupied region near the bottom of the conduction band, the states arise mainly from the 3*p*, 4*p*, 5*p,* and 6*p* orbitals of Si, Ge, Sn, and Pb atoms, respectively. In addition some unoccupied *np* states of Cl, Br, and I (*n* = 3, 4, and 5, respectively) are also present. The presence of *p* partial DOS of the Si/Ge/Sn/Pb atoms in the unoccupied region and its low DOS in the occupied region indicate charge transfer from these atoms.

The band structures of Si_2I_2PN, Ge_2I_2PN, Sn_2I_2PN, and Pb_2I_2PN double helices are shown in **Fig. 5** as representatives while for other cases the results are given in **Fig. S4** in Supplementary Information. In all the cases, the double helices are semiconductors and the bands near the top of the valence band and the bottom

of the conduction band show good dispersion. *It is interesting to note that Sn_2I_2PN and Pb_2I_2PN are direct band gap semiconductors* while for Si_2I_2PN direct and indirect transitions are equally probable since the bands at the Γ and X have the same energy. For Ge_2I_2PN the most preferred transition is X to Γ and hence it is an indirect band gap semiconductor. Note that for SnIP, the band gap is indirect and the direct band gap is slightly higher.

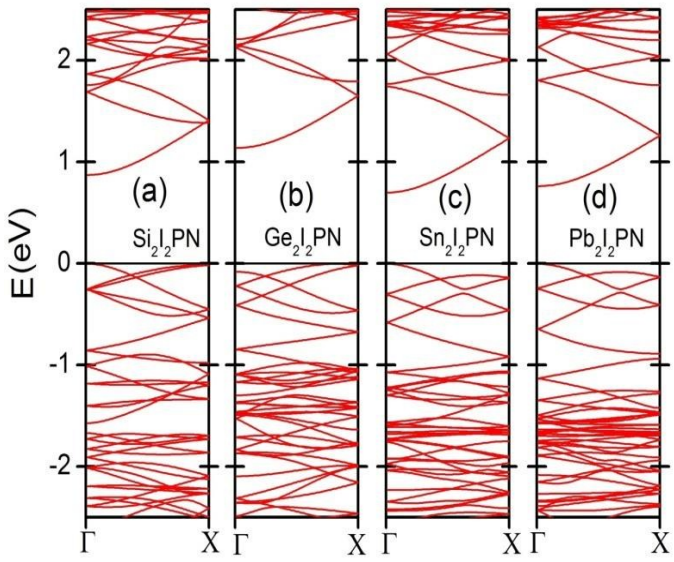

Fig. 5. Electronic band structures of various A_2B_2PN double helices. The top of the valence band has been taken as reference for energy.

The total and angular momentum resolved partial DOSs of A_2B_2SiS double helices (**Fig. 6**) show that these are also semiconductors and Ge_2I_2SiS has the highest band gap of 1.30 eV in this category. Here too the *p* levels of the A atoms from the outer helix dominate the conduction band region. This is due to the charge transfer from the A atoms to nearby halogens and SiS chain. A few unoccupied *p* states of halogens are also present in the conduction band. In the valence band region near the top of the band we find *p* states from both these atoms of the outer helix while their *s* states lie far below the top of the valence band. The calculated band structures of these double helices are shown in **Fig. 7**. *These results demonstrate that Sn_2Br_2SiS and Pb_2Br_2SiS are direct band gap semiconductors* whilst the remaining double helices are indirect band gap semiconductors.

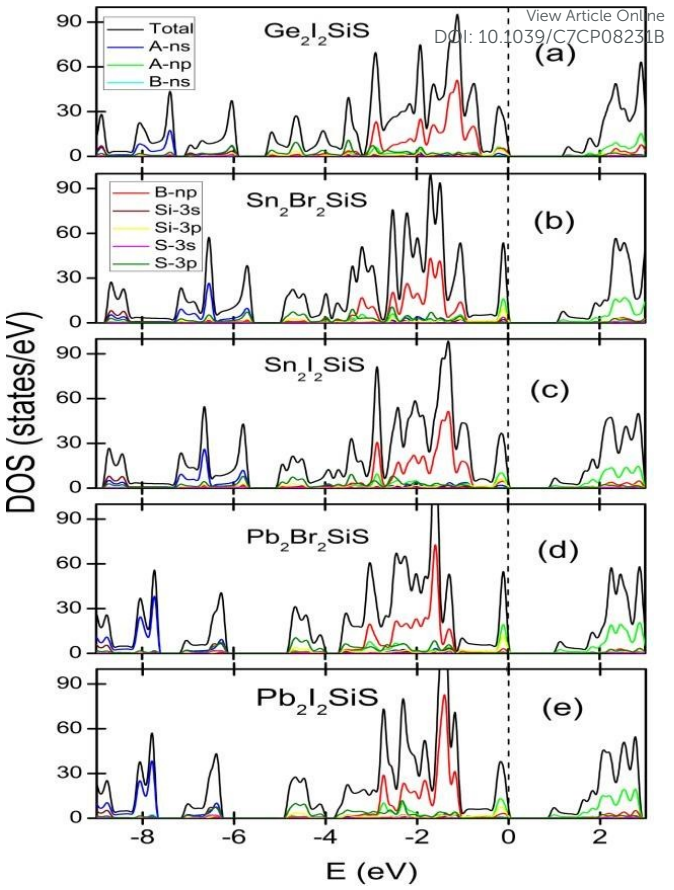

Fig. 6. The total and angular momentum resolved partial electronic density of states of various A_2B_2SiS double helices. The vertical broken line shows the top of the valence band.

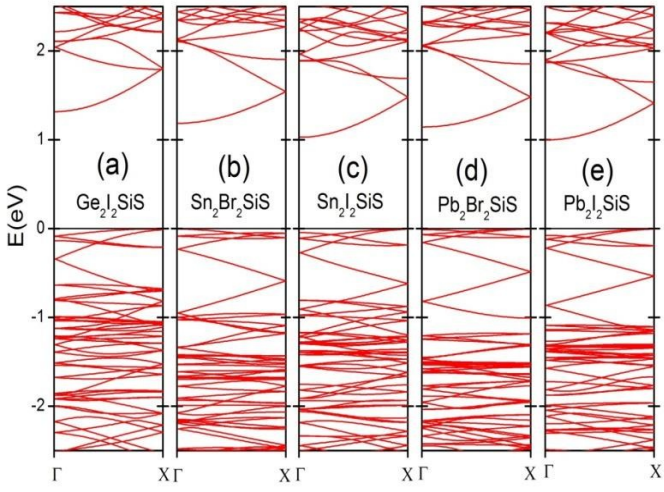

Fig. 7. The energy bands of various A_2B_2SiS double helices in the vicinity of the top (bottom) of the valence (conduction) band. The top of the valence band has been taken as reference for energy.

Figures 8 and **9** show the partial charge density plots in the case of Sn_2I_2PN and Sn_2I_2SiS helices, respectively. In both the cases one can see the charge density arising from the *p* orbitals of I and Sn atoms in the valence band energy region while in the conduction band energy region the contribution is mainly from the *p* orbitals of Sn. Also in the case of Sn_2I_2PN one can see from **Fig. 8(d)** some overlap between the densities arising from the *p* orbitals in successive turns of the outer helix.

Further calculations have been performed on bond order and sum of the bond orders for different atoms in all double helices using DDEC6 analysis. These results are given in Table 3. It is noted that in the case of double helices with P atoms in the inner helix, the sum of the bond order for P atoms is very close to 4 while for double helices with Si atoms in the inner helix the sum of the bond order is slightly lower with the value of about 3.6. These are the largest values and agree with four covalent bonds that each of these atoms forms. Also the bond order for the PN as well as SiS bond in the inner helix is close to 1 suggesting covalent bond character. The sum of the bond orders for N and S atoms is around 3.1 while for the A atoms the sum of the bond orders is close to 2 and for B atoms the value is about 1.2. These results also suggest the importance of the inner helix in the stability of the double helices due to strong covalent bonding.

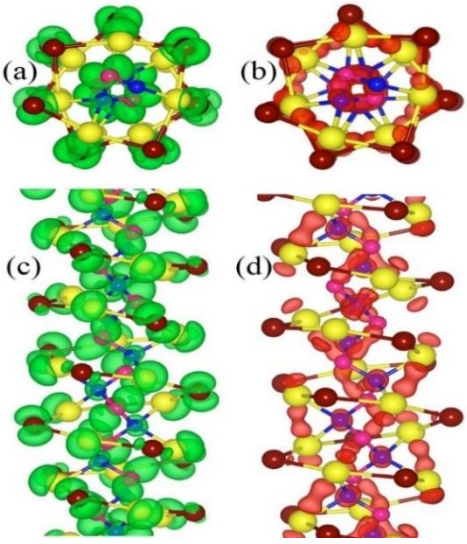

Fig. 8. Top and side views of the partial charge density plot in (a) and (c) in the valence band (-1.0 eV to 0.0 eV) region, (b) and (d) in the conduction band (0.6 eV to 1.6 eV) region, respectively, for Sn_2I_2PN. Weak interaction can be seen between the *p* orbitals on Sn atoms in (d).

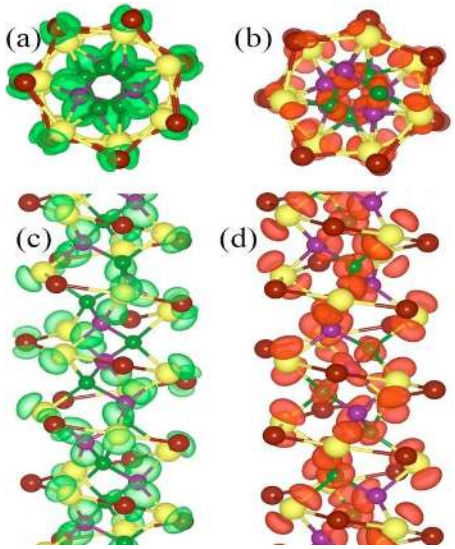

Fig. 9. Top and side views of the partial charge density plot in (a) and (c) in the valence band (-1.0 eV to 0.0 eV) region, (b) and (d) in the conduction band (0.8 eV to 1.8 eV) region, respectively, for Sn_2I_2SiS.

Table 3. The average values of bond order (BO) and sum of the bond orders (SBO) of various bonds and atoms present in the inorganic double helices A_2B_2XY obtained by using DDEC6 analysis. For reference values for SnIP are also given.

System A_2B_2XY	BO (A-B)	BO (A-X)	BO (A-Y)	BO (X-Y)	SBO (A)	SBO (B)	SBO (X)	SBO (Y)
SnIP	0.43	0.59	-	0.99	2.33	1.30	3.67	-
Si_2I_2PN	0.48	0.64	0.60	0.85	2.82	1.60	3.94	3.18
Ge_2Br_2PN	0.42	0.57	0.47	0.98	2.33	1.31	4.0	3.17
Ge_2I_2PN	0.42	0.57	0.47	0.98	2.42	1.41	4.0	3.16
Sn_2Cl_2PN	0.42	0.55	0.43	1.05	2.27	1.21	4.0	3.16
Sn_2Br_2PN	0.43	0.54	0.41	1.05	2.34	1.28	4.0	3.16
Sn_2I_2PN	0.43	0.55	0.40	1.06	2.40	1.36	4.0	3.14
Pb_2Cl_2PN	0.38	0.51	0.36	1.12	2.03	1.09	4.06	3.20
Pb_2Br_2PN	0.39	0.50	0.36	1.12	2.09	1.15	4.06	3.19
Pb_2I_2PN	0.40	0.50	0.37	1.10	2.20	1.28	4.08	3.18
Ge_2I_2SiS	0.42	0.72	0.56	0.78	2.34	1.39	3.67	3.20
Sn_2Br_2SiS	0.42	0.67	0.50	0.85	2.23	1.22	3.57	3.11
Sn_2I_2SiS	0.43	0.68	0.49	0.85	2.31	1.33	3.60	3.10
Pb_2Br_2SiS	0.37	0.62	0.45	0.90	2.01	1.10	3.55	3.10
Pb_2I_2SiS	0.40	0.62	0.43	0.91	2.10	1.21	3.58	3.08

DOI: 10.1039/C7CP08231B

We further studied the effects of doping on the electronic structure of these stable double helices by considering Sn_2I_2PN double helix and doped the inner PN helix substitutionally with Si and S atoms. Since Si is one electron deficient in its valence shell compared with P/N, the substitution of a Si atom corresponds to hole doping while the substitution of S atom will result in electron doping due to the presence of one extra valence electron on S. We doped Si and S on both P and N sites to explore which one is more favourable. But for both P and N sites, S doped double helix undergoes structural debacle. Therefore, we concluded that S doping is structurally not favourable. For Si doping, even though Si at N site yields a distorted helix, the P site is found to be the most suitable one since there is no noticeable distortion. The atomic structure as well as the electronic band structure and DOS for the Si doped double helix are shown in **Fig. 10**. From these results we confirmed that the Si doped double helix is metallic in nature due to the presence of one partially occupied band which crosses the E_f.

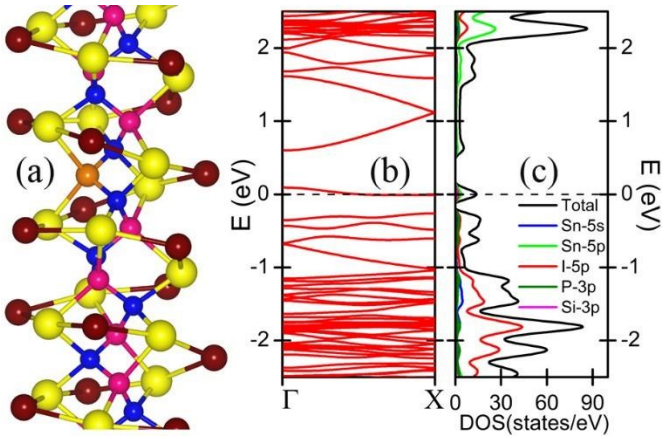

Fig. 10. (a) Optimized atomic structure of Si doped Sn_2I_2PN double helix along with its (b) electronic band structure and (c) total (black curve) and partial (red – iodine 5*p* and green – Sn 5*p* are dominant in the energy range shown) DOS. Brown and yellow balls represent I and Sn atoms in the outer helix while orange, blue, and pink balls show Si, P, and N atoms in the inner helix, respectively. The Fermi energy is taken to be the reference for energy.

Conclusions

In summary, we have performed first principles calculations to understand the structural and electronic properties of A_2B_2PN and A_2B_2SiS inorganic double helices with A = Si, Ge, Sn, and Pb and B = Cl, Br, and I. These systems and also the previously studied SnIP type systems have two quite different length scales: (1) a short one for the inner helix and (2) a much longer one in the outer helix while the bond lengths between the two helices lie in the intermediate range. The difference between the two lengths could be astonishingly up to about 80%. This is much larger than about 15% difference in atomic radii for forming alloys in multicomponent systems. This seems to be a reason that there are two different helices which coexist by interlinking. Also a facilitating factor is that there is some flexibility in the outer helix as we find from the variation of up to 17% in the ratios of the bond lengths in the outer and inner helices in different systems but the flexibility is less in bond angles. The Sn-I-Sn type bond angles have up to ~10% variation around the mean value of 100° while I-Sn-I angles have up to ~6% deviation with the mean value of ~158°. On the other hand P-N-P or Si-S-Si angles in the inner helix have only 2% deviation with the mean value of 101°, while N-P-N or S-Si-S angles have a larger deviation of 7% around the mean value of 96°. Accordingly, the outer helix has more flexibility while the inner helix has strong covalency with less deviation in bond angles. These results are supported from the calculations of bond order.

Our calculations reveal that among the A_2B_2PN helices, bromides and iodides of Ge, Sn, and Pb as well as Si_2I_2PN and Pb_2Cl_2PN form structurally stable double helices. Also, we find structurally stable double helices of Ge_2I_2SiS, Sn_2Br_2SiS, Sn_2I_2SiS, Pb_2Br_2SiS, and Pb_2I_2SiS which are symmetric. These results indicate that SiS inner helix which is isoelectronic to P is a suitable candidate for replacing the P helix of the previously reported inorganic SnIP double helix and related systems. In contrast to the previously reported double helices, where the inner helix of P is covalently bonded, here we have reported new double helices in which the core helix has partially polar character. We believe that the experimental realization

PCCP ARTICLE

View Article Online
DOI: 10.1039/C7CP08231B

of the double helices with PN inner helix could be achieved by growing halides of group 14 elements on linear inorganic PN polymers. In addition, SiS is another possible alternative for P helix of the inorganic double helices. These double helices are semiconducting and A_2I_2PN (A = Si, Sn, and Pb) as well as A_2Br_2SiS (A = Sn and Pb) have a direct band gap. We have further demonstrated that the electronic properties of the A_2B_2PN double helices can be varied by doping such as with Si. We find that hole doping is most favourable in these systems. We hope that the present work will open up new avenues for experimentalists to design a variety of functional inorganic double helices for multifarious applications.

Conflicts of interest

There are no conflicts of interest to declare.

ACKNOWLEDGMENT

TKB gratefully acknowledges hospitality at the Dr. Vijay Kumar Foundation. The calculations were performed on the high performance computing facility Magus of Shiv Nadar University and at CECRI, Karaikudi.

Notes and references

1. J. D. Watson and F. H. C. Crick, , *Nature,* 1953**, 171**, 737-738.
2. H. Huang, S. Hong, J. Liang, Y. Shi, and J. Deng, *Polymer Chem.,* 2017, **8**, 5726-5733.
3. Y. Furusho and E. Yashima, *J. Polymer Sci. Part A: Polymer Chem.,* 2009, **47**, 5195-5207.
4. E. Yashima, K. Maeda and Y. Furusho, *Acc. Chem. Res.,* 2008, **41**, 1166-1180.
5. D. Pfister, K. Schäfer, C. Ott, B. Gerke, R. Pöttgen, O. Janka, M. Baumgartner, A. Efimova, A. Hohmann, P. Schmidt, S. Venkatachalam, L. van Wüllen, U. Schürmann, L. Kienle, V. Duppel, E. Parzinger, B. Miller, J. Becker, A. Holleitner, R. Weihrich and T. Nilges, *Adv. Mater.,* 2016, **28**, 9783-9791.
6. X. Li, Y. Dai, Y. Ma, M. Li, L. Yu and B. Huang, *J. Mater. Chem. A,* 2017, **5**, 8484-8492.
7. M. Baumgartner, R. Weihrich and T. Nilges, *Chemistry – A European Journal,* 2017, **23**, 6452-6457.
8. W. Ju, H. Wang, T. Li, H. Liu and H. Han, *RSC Adv.,* 2016, ***6***, 50444-50450.
9. A. S. Ivanov, A. J. Morris, K. V. Bozhenko, C. J. Pickard and A. I. Boldyrev, *Angew. Chem. Int. Ed.,* 2012, **51**, 8330-8333.
10. A. S. Ivanov, T. Kar and A. I. Boldyrev, *Nanoscale*, 2016, **8**, 3454-3460.
11. C. W. Allen, *Coord. Chem. Rev.,* 1994, **130**, 137-173.
12. I. Haiduc, *Encyclopedia of Inorganic Chemistry*, John Wiley & Sons, Ltd: 2006.
13. H. R. Allcock, D. C. Ngo, M. Parvez, R. R. Whittle and W. J. Birdsall, *J. Am. Chem. Soc..,* 1991**, 113**, 2628-2634.
14. Z. Zhu, J. Guan, D. Liu and D. Tománek, *ACS Nano*, 2015, **9**, 8284-8290.
15. A. K. Deb and V. Kumar, Phys. Stat. Sol. (b), 2016, **254**, DOI 10.1002/pssb.201600379.
16. H. Jiang, T. Zhao, Y. Ren, R. Zhang and M. Wu, *Science Bulletin*, 2017, **62**, 572-578.
17. H. R. Jiang, T. S. Zhao, M. Liu, M. C. Wu and X. H. Yan, *J. Power Sources*, 2016, **331**, 391-399.
18.P. E. Blöchl, *Phys. Rev. B*, 1994, **50**, 17953-17979.
19.G. Kresse and D. Joubert, *Phys. Rev. B*, 1999, **59**, 1758-1775.
20. G. Kresse and J. Furthmuller, *Phys. Rev. B,* 1986, **54** 11169-11186.
21. J. P. Perdew, J. A. Chevary, S. H. Vosko, K. A. Jackson, M. R. Pederson, D. J. Singh and C. Fiolhais, *Phys. Rev. B*, 1992, **46**, 6671-6687.
22. A. Tkatchenko and M. Scheffler, *Phys. Rev. Lett.,* 2009, **102**, 073005.
23. T. Bučko, S. Lebègue, J. Hafner, and J. G. Ángyán, *Phys. Rev. B*, 2013, **87**, 064110.
24. J. P. Perdew, K. Burke and M Ernzerhof, *Phys. Rev. Lett.,* 1996, **77** 3865-3868.
25. G. Henkelman, A. Arnaldsson and H. Jónsson, *Comput. Mater.Sci.*, 2006, **36**, 354-360.
26. R. F. W. Bader, P. J. MacDougall, and C. D. H. Lau, *J. Am. Chem. Soc*., 1984, **106,** 1594-1605.
27. T. A. Manz, *RSC Adv.*, 2017, **7**, 45552–45581.
28. T. A. Manz and N. Gabaldon Limas, *RSC Adv.*, 2016, **6,** 47771-47801.

ARTICLE PCCP

View Article Online
DOI: 10.1039/C7CP08231B

TOC Graphic

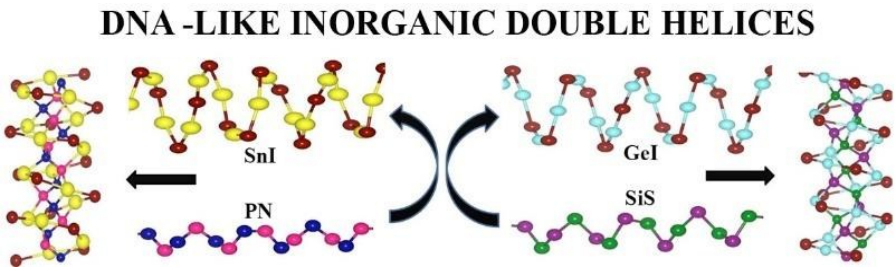

Caption: The inner (PN or SiS) and outer (SnI and GeI) helices forming the Sn_2I_2PN and Ge_2I_2SiS inorganic double helices.